



Surfaces Affect Screening Reliability in Formulation Development of Biologics

Mitja Zidar¹ · Gregor Posnjak² · Igor Muševič^{2,3} · Miha Ravnik^{3,2} · Drago Kuzman¹

Received: 12 May 2019 / Accepted: 8 November 2019 / Published online: 6 January 2020
© Springer Science+Business Media, LLC, part of Springer Nature 2020

ABSTRACT

Purpose The ability to predict an antibody's propensity for aggregation is particularly important during product development to ensure the quality and safety of therapeutic antibodies. We demonstrate the role of container surfaces on the aggregation process of three mAbs under elevated temperature and long-term storage conditions in the absence of mechanical stress.

Methods A systematic study of aggregation is performed for different proteins, vial material, storage temperature, and presence of surfactant. We use size exclusion chromatography and micro-flow imaging to determine the bulk concentration of aggregates, which we combine with optical and atomic force microscopy of vial surfaces to determine the effect of solid-liquid interfaces on the bulk aggregate concentration under different conditions.

Results We show that protein particles under elevated temperature conditions adhere to the vial surfaces, causing a substantial underestimation of aggregation propensity as determined by common methods used in development of biologics. Under actual long-term storage conditions at 5°C, aggregate particles do not adhere to the surface, causing an increase in bulk concentration of particles, which cannot be predicted from elevated temperature screening tests by common methods alone. We also identify specific protein – surface interactions which promote oligomer formation in the nanometre range.

Conclusions Special care should be taken when interpreting size exclusion and particle count data from stability studies if different temperatures and vial types are involved. We propose a novel combination of methods to characterise vial surfaces and bulk solution for a full understanding of protein aggregation processes in a sample.

KEY WORDS adhesion · aggregation · monoclonal antibodies · pharmaceutical development · sedimentation · solid-liquid interface

ABBREVIATIONS

AFM	Atomic force microscopy
ECD	Equivalent circular diameter
GuHCl	Guanidine hydrochloride
mAb	Monoclonal antibody
MFI	Micro-flow imaging
MWCO	Molecular weight cutoff
PETG	Polyethylene terephthalate glycol
PS80	Polysorbate 80
SEC	Size exclusion chromatography
UPW	Ultrapure water

INTRODUCTION

Therapeutic proteins and monoclonal antibodies (mAbs) are increasingly used for treatment of various adverse conditions – such as cancer, autoimmune diseases and life-threatening infections. A fundamental challenge in developing therapeutic formulations is ensuring their stability in an aqueous solution as proteins are inherently labile molecules that often undergo unwanted chemical or physical degradation during manufacturing and storage (1–5). In particular, aggregation is a

✉ Drago Kuzman
drago.kuzman@novartis.com

¹ Novartis Global Drug Development/Technical Research & Development, Technical Development Biosimilars, Lek Pharmaceuticals d. d., Kolodvorska 27, Mengeš, Slovenia

² Jožef Stefan Institute, Jamova 39, 1000 Ljubljana, Slovenia

³ Faculty of Mathematics and Physics, University of Ljubljana, Jadranska 19, 1000 Ljubljana, Slovenia

commonly observed degradation pathway of therapeutic protein drug products, potentially causing adverse effects by enhancing product immunogenicity (6). Therefore, the content of larger subvisible and visible aggregates is limited by United States and European regulatory agencies, but notably also smaller oligomers composed of native-like monomers were shown to be capable of triggering an unwanted immune response (7). Analysis of aggregates in the whole size range from smaller aggregates in the range of nanometers to larger particles in the range of micrometers and millimeters is thus crucial in determining the formulation stability and safety.

In addition to the inherent aggregation propensity due to unique amino acid sequence, protein aggregation in an aqueous solution also depends on a variety of environmental conditions, such as temperature, pH, solution composition and container type (8). Numerous studies have identified various aggregation mechanisms in bulk solution under different stress conditions – thermal, mechanical, freeze/thaw (9–15), with a range of models based on the Smoluchowsky coagulation equation approach (16–18). Such models are of crucial importance because they provide insight into the shelf-life stability of the final product.

The effect of interfaces on protein solutions has also been thoroughly investigated. Native proteins were found to adhere to the air-liquid interface and the resulting film properties were studied with the use of a Langmuir trough (19,20). The rate of adsorption to the air-liquid interface was found to directly correlate to the aggregation rate during shaking stress (21). Surface rupture and subsequent detachment of the protein film was identified as a major cause of aggregate formation (22). Similarly, proteins were also found to adsorb on liquid-solid interfaces, with abrasion or rinsing of adsorbed protein leading to subvisible aggregate formation (23,24). Formation of protein monolayers in absence of additional stress was studied rigorously with diverse methods such as atomic force microscopy and neutron interference (25,26). These processes, together with cavitation, are of major importance when studying the stability of formulated protein pharmaceuticals during mechanical stress (27,28). Formation of larger aggregates can, under most conditions, be prevented with the use of surfactants. However, surfactants and their degradation products can cause chemical and structural degradation of protein molecules. Therefore, the surfactant concentration has to be balanced between the desirable aggregation prevention and detrimental structure-perturbation effects (29).

In this work, we demonstrate the effect of glass and PETG container surfaces on the process of aggregation under elevated temperature and long-term storage conditions in the absence of mechanical stress. Effectively, we observe that the surface affected aggregation relative to the bulk aggregation propensity is varied by using different vial fill volumes, resulting in different side and bottom surface to volume ratios,

where the contribution of the top air-liquid interface is kept equivalent in all studies (i.e. exhibits stable coating with protein monomers) (19–22). We studied three different mAbs of type IgG1. Specific interactions due to container material were identified by using glass and PETG containers. Effect of surfactant (PS80) was also studied. These materials are commonly in use in biopharmaceutical industry. Vials with protein solution were subjected to elevated temperature and the ensuing aggregation was measured by size exclusion chromatography and flow imaging microscopy. The vials were then gently rinsed multiple times and checked for protein surface adhesion with optical and atomic force microscopy. Different mechanism of protein-vial interactions were identified, including diffusion-driven coating of the vial surface with protein material, sedimentation-driven adhesion of micron-sized and larger particles to the vial bottom and promotion of surface-induced aggregation in the sub-micron range. Protein monomers and smaller aggregates (sub-100 nm) measured by size exclusion are interpreted as homogeneously distributed colloidal particles. In contrast, micron sized and larger particles, measured by flow imaging microscopy, behave as sedimenting particles. The work presented focuses on long-term storage of proteins specifically from the view of protein aggregate interaction with the liquid-vial interface. We conclude that the current array of methods commonly used in the pharmaceutical industry is insufficient under certain conditions, especially in combination with elevated temperature conditions. A novel combination of methods is proposed which we show can greatly assist in the interpretation of results from time and resource consuming stability screenings in the biopharmaceutical industry.

MATERIALS AND METHODS

Materials

Three monoclonal IgG1s (mAb 1, mAb 2 and mAb 3, with isoelectric points between pH 8 and pH 9) in different formulations at different concentrations (27–63 mg/ml) were provided by Lek Pharmaceuticals d.d. MAb 2 and 3 were dialyzed in Slide-A-Lyser Dialysis Cassettes (10,000 MWCO, 12–30 ml capacity) to 25 mM sodium citrate, pH 6.5, with a buffer to sample volume ratio of approximately 50:1. MAb 1 was already provided in this buffer. After dialysis, all the protein solutions were further diluted to 25 mg/ml with citrate buffer. A stock solution of PS80 (Sigma) at 0.1% w/w was prepared and added (dilution factor of 50) to half of each solutions resulting in 6 different formulations – three different IgGs at 25 mg/ml in 25 mM sodium citrate buffer at pH 6.5 with and without 0.02% added PS80. All the

formulations were filtered through a vacuum pump-driven 0.22 μm filter.

Stressing of the IgG Formulations

Glass (Nipro 83657 mirror ground injection crimp top bottles) and PETG (Thermo Scientific™ Nalgene™ PETG Diagnostic Bottles with Closure) vials were used. Glass vials were sprayed on the inside with 70% isopropanol and left to dry at 55°C for 2 h. PETG vials were provided sterile. The quality of glass vials (FIOLAX® klar borosilicate glass) is HGB 1 according to ISO 719, making them suitable both for primary packaging of biopharmaceutical products on the market and stress stability studies at elevated temperature. Both used materials or their equivalents are in contact with most of the biopharmaceutical products throughout their lifecycle.

Sets of five vials from both materials were filled with different volumes of prepared formulations as shown in Fig. 1. The volumes for glass/PETG vials were the following: 1.5/1.8 ml (V1), 3.0/3.6 ml (V2), 4.3/5.1 ml (V3), 6.0/7.1 ml (V4), 10.0/11.9 ml (V5), resulting in equal liquid levels for glass and PETG vials. Each measurement point for every mAb consisted of four sets of five identical vials. The different sets of vials were: (i) PETG vials filled with formulation without surfactant, (ii) PETG vials filled with formulation with added surfactant, (iii) glass vials filled with formulation without surfactant and (iv) glass vials filled with formulation with added surfactant. The vials were then subjected to 40°C, stationary throughout the experiment. This ensured that aggregation did not occur due to disturbance of air/liquid or liquid/vial interface and that only the static long-term contribution of the surfaces was investigated. After elevated temperature conditions, some mAb 1 samples with micron-sized and larger aggregates present in bulk were transferred into fresh vials and stored at 5°C for a month to study the interaction between already formed aggregates and clean vial surface at storage conditions. All the other samples were stored at 5°C after elevated temperature stress directly.

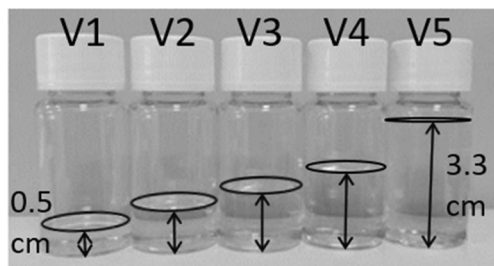


Fig. 1 Vial fill volumes. Sets of five vials V_i were filled with different volumes to determine the effect of different surface to volume ratio. PETG (in the figure) and glass vials were filled according to vial sizes, resulting in the same liquid level heights (bolded) in sets of vials from both materials.

Micro-Flow Imaging (MFI)

A Micro-Flow Imaging system (MFI5100, ProteinSimple), equipped with a silane-coated flow cell (400 μm , 1.6 mm) and controlled by the MFI View System Software (MVSS) version 2 was used for flow imaging microscopy analysis. The system was flushed with 5 ml of ultrapure water (UPW) from UltraPURELAB® Chorus 2 water system before each measurement. The background particle count was determined by flowing UPW. Before measurement, samples were opened, degassed at 950 mbar for 20 min and homogenized (rotated 10 times over the cap). 1.5 ml of each sample was pipetted out of the vial and analyzed at a flow rate of 0.2 ml/min and a camera frame rate of 3 frames per second. Flow cell was flushed with 0.7 ml of pre-run sample volume, and the remaining 0.7 ml was analysed. The diameter of a sphere with the same cross-section area as the particle (equivalent circular diameter - ECD) was calculated by the software from all the images for all the measured particles and presented as a measure of particle size.

Size Exclusion Chromatography (SEC)

Samples were analysed at 40°C on a Waters ACQUITY UPLC System with a SEC column (200 Å pore size, 1.7 μm bead size and 4.6 mm \times 150 mm column dimensions). Sample load volume was 0.75 μl . The mobile phase (50 mM sodium dihydrogen phosphate and 400 mM sodium perchlorate, pH 6.0) flow rate was 0.4 ml/min with a total run time of 5 min per sample. Samples were diluted to 1 mg/ml in 150 mM sodium phosphate, pH 7, and held at 2–8°C in the auto-sampler prior to injection. The chromatograms were analyzed with Empower 3 software. All the peaks eluting before the main peak, corresponding to the native protein, were designated as aggregates. Their relative areas were summed and presented as the total relative amount of aggregates.

Optical Microscopy

Solution in vials chosen for optical microscopy was homogenized (rotated 10 times) and poured out. The residual solution was then removed by rinsing (also rotating 10 times) the vials three times with.

5 ml of UPW to prevent any deposition because of drying of the protein solution. The insides of the vials were blown out with compressed nitrogen until dry and the vials were broken into small pieces.

Optical microscopy of the inner vial surfaces was performed on a Nikon Eclipse E-100 microscope with epi illumination with 10 \times and 20 \times objectives. The images were acquired with a Canon EOS 550D digital camera with a 2.26 \times magnification tube. Breaking of the glass vials into smaller pieces, suitable for optical microscopy, resulted in glass

shards being present on the samples, which could not be blown off by compressed nitrogen. These glass shards are easily recognized in the micrographs by their sharp edges in contrast to the softer borders of the aggregates. Several pieces of each vial were examined with the optical microscope by scanning their surface and representative images for each sample were chosen for inclusion in the article. Several different blanks were examined to verify the cause of the deposits: clean vials, vials with buffer solution and vials with native unstressed protein. In none of these cases any noticeable deposits were present.

Atomic Force Microscopy (AFM)

To additionally characterize the deposits seen in optical microscopy, surfaces of glass vials were examined by atomic force microscopy (AFM). The preparation procedure was the same as in the case of optical microscopy. AFM measurements were conducted on Digital Instruments Nanoscope IIIa in tapping mode with silicon Olympus Micro Cantilevers (resonant frequency 300 kHz, spring constant 26 N/m). Thickness of the deposited material was determined by measuring the height of a step, produced by gently running the tip of a scalpel over the glass, which removed the adhered protein material in a narrow strip. The results presented in the article are averages of measurements on several different pieces of a vial of each sample. Only the results from glass vials are presented because the plastic vials proved impossible to measure after breakage, most likely because the plastic pieces accumulated some static electric charge during breakage and interacted with the AFM tip.

Recovery and Quantification of Adhered Protein

A set of vials was additionally selected for quantification of adhered protein. 0.5 ml of 8 M guanidine hydrochloride (GuHCl) in UPW was added to rinsed vials and incubated overnight at room temperature on a rotator such that GuHCl could access all of the vial wall surface. The amount of recovered protein was determined next day by measuring the absorbance at 280 nm using an Eppendorf BioSpectrophotometer basic. Absorbance value of GuHCl solution in a fresh vial following the same treatment was used as a blank measurement.

RESULTS

Adhesion of Aggregate Particles

Representative pictures of the vial bottoms, taken from elevated temperature conditions are presented in Fig. 2 as determined by AFM. Both mAb 1 and 2 vials contain randomly

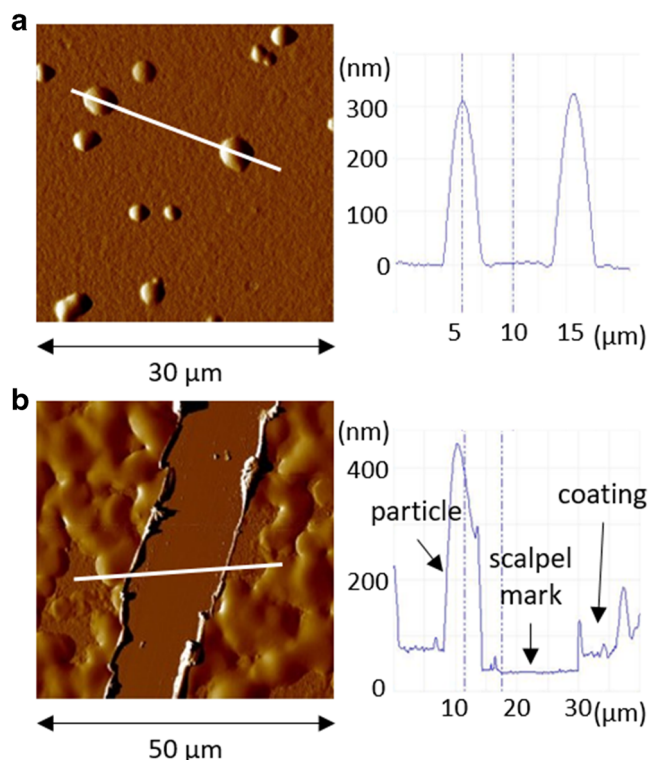


Fig. 2 Adhesion of particles at the bottom of glass vials, as seen by AFM. The images on the left show the cantilever oscillation amplitude and the graphs on the right show height of the surface features along the white lines. **(a)** MAb 1 V3 sample after 14 days – individual micron-sized particles can be clearly distinguished from the smooth coating. The protein particles at the surfaces are several hundred nanometers high (aspect ratio of approximately 10:1). **(b)** MAb 2 V5 sample after 2 months – micron-sized particles are densely strewn on top of the coating and mostly overlap. The scalpel mark used to determine the coating thickness (around 30 nm) is clearly visible.

distributed lumps on the vial surface, around 1–5 µm in diameter and 100–500 nm in height. These lumps are not present in vials containing blank samples (UPW, buffer or non-stressed protein), but otherwise treated the same as vials with samples. Vials with protein after elevated temperature stress are the only vials containing these lumps, with protein type as the only parameter affecting their size, number and distribution. Therefore we interpret these lumps as sedimented and adhered larger particles (aggregates). The aspect ratio of the particles is approx. 10:1 (diameter:height), which can be explained by collapse of particles during drying, as water occupies a large fraction of the protein particle volume (30). The particles observed with AFM are also visible with optical microscopy (Fig. 3). The figure also shows the surface concentration gradient of these particles with position on the vial, further showing that the lumps observed with AFM represent adhered sedimented particles from bulk. Note that any artefacts caused by drying of the vials would be evenly distributed on vial bottom and walls following the blow drying of the vials. Because of vial rinsing prior measurement, the material is truly adhered and not only sedimented on the bottom.

In addition to the randomly distributed sedimented particles, all three mAbs under 40°C temperature conditions form a uniform coating of varying thickness (Fig. 4) of dry protein material on the glass surface. This thickness is measured by scraping a line along the bottom with a scalpel as seen in Fig. 2b. Thickness of the coating as measured by AFM is relatively independent from the vial filling volume, suggesting that the deposition of material to this coating is mostly diffusion driven. In all cases, the thickness of the uniform layer is greater than 10 nm, much thicker than a possible single layer of mAb molecules.

Total mass of adhered protein was estimated by recovery with GuHCl. The results from a representative set of vials are in Table I. The set contains both glass and PETG vials and several samples measured in both vial types as controls. Based on the blank measurements, the estimated error for the values in the table is 0.02 mg. The ranking by mass is in line with the AFM measurements, with the highest recovered mass in the mAb 2 sample after 2 months of temperature stress. Little to no protein material desorbed from mAb 3 vials exposed to similar stress, with the mass of recovered mAb 2 after a shorter stress in between. The average surface coverage with protein material as estimated from this experiment ranges from less than 1 $\mu\text{g}/\text{cm}^2$ to 10 $\mu\text{g}/\text{cm}^2$, depending on protein type and duration of temperature stress. The glass and PETG vial measurements are very much in line, gaining insight also into the particle adsorption to the PETG vials, suggesting that adsorption is mostly independent of the tested vial materials. The absolute measured protein mass represents less than 1 % of the total protein material in the vials and its deficit is therefore impossible to detect by bulk measuring methods such as SEC.

Sedimentation and Surface Saturation by Selected Proteins

To test the influence of solid/solution interface on protein aggregation we expose samples with different surface-to-volume ratios to elevated temperature. After 2 weeks at 40°C, mAb 1 shows a significant increase in the number of particles ($>2 \mu\text{m}$) as detected by MFI, with the particle concentration strongly dependent on the vial filling volume (i.e. surface to bulk ratio). Note that for mAb 2 and 3, the

concentration of particles in the bulk under the elevated temperature conditions showed no clear trend, remained constant or even decreased. For mAb1, in the vials filled with the largest sample volume in the absence of surfactant, the number of particles is already increasing after a week of elevated temperature conditions, while the vials filled with lower volume remain essentially particle-free at first, with a sharp increase in particle concentration at a certain time (Fig. 5). The lowest volume accumulated little to no particles. The results are quantitatively equal in both glass and plastic vials. The experiment was repeated again in PETG vials filled with slightly different volumes for a longer period of time (30 days), again yielding the same trend. Due to the similarity of results, only one run (PETG vials, 19 days) is presented in Fig. 5.

A simple model can qualitatively explain this behavior of surface affected aggregation. The model assumes continuous and homogeneous particle formation with time t in bulk with the rate a (number of formed particles per millilitre per day). The total number of formed particles is therefore the rate multiplied by time and sample volume. The linear increase of particles with time is indeed only a rough estimate, drawing from the fact that Smoluchowsky type models generally predict such a linear increase of total aggregate content over time under static conditions (31). These particles sediment and adhere to the bottom of the vials - as detected by AFM - but only until the bottom with surface area S_b (square centimetres) is covered by a surface concentration of adhered particles η (number of particles per square centimetre). These particles are removed from the bulk, and their total number is the vial bottom surface area times surface concentration. In equilibrium, the expression for the total number of particles N in the bulk of the sample based on this model is:

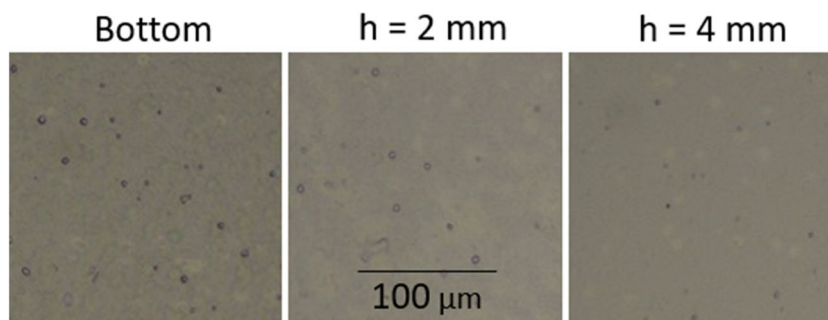
$$N = aVt - \eta S_b$$

By dividing the expression with the volume of the vial, and taking into account the cylindrical geometry of the vial, we get an expression for the particle concentration in the bulk:

$$c = at - \eta/h,$$

where $c = N/V$ is the particle concentration (number per millilitre) and h is the height of the liquid level in the vial. This

Fig. 3 Difference in the size of surface-adhered particles as seen with optical microscopy, taken at different heights, measured from the bottom of the vial.



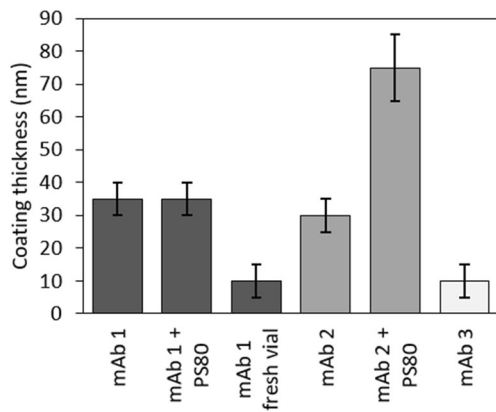


Fig. 4 Thickness of protein material deposited on the bottom of glass vials, as measured with AFM. mAb 1 was measured after 2 weeks, and mAbs 2 and 3 after 2 months of exposure to 40°C. One mAb 1 sample was transferred after the elevated temperature conditions into a fresh vial and measured after storing for 1 month at 5°C. The thickness of the protein material coating on the vial bottom is independent of the vial fill volume (and the cumulative aggregate content in the vial).

equation represents a constant rate of particle concentration increase *a* with time, but only after a certain time, which depends on the height of the vial *h*. The equation is represented by a straight line in the graph of particle concentration *c* versus reciprocal liquid level *l/h* with the initial value of *at* and the slope of $-η$, which is measurable by AFM. Both data representations are shown in Fig. 5. The final surface concentration of particles as determined by fitting the model gives $η \sim 4 \times 10^5$ particles per square centimetre. Indeed, this value is well supported by optical microscopy and AFM, which show roughly 5×10^5 of particles per square centimeter larger than 2 μm adhered to the bottom, as estimated from Figs. 2a and 6.

A basic estimate of sedimentation velocity of protein particles can be performed to qualitatively check the model validity. Assuming a spherical shape of the aggregate particles, there are three forces acting on the particle: gravity, lift, and Stokes drag. This equilibrium can be written as

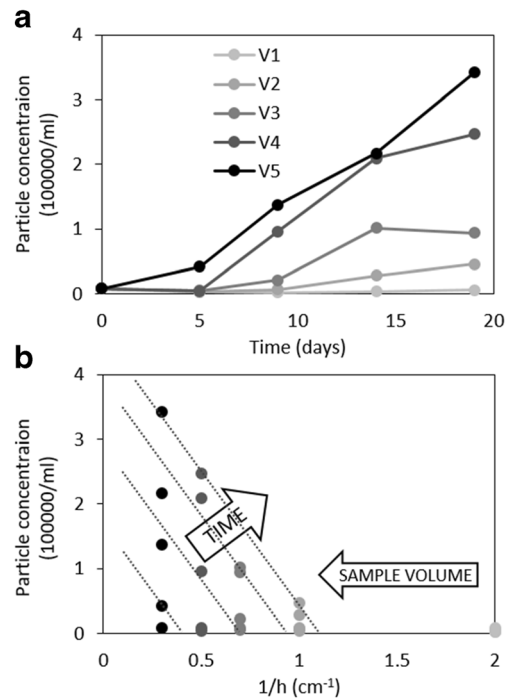


Fig. 5 Schematic representation of the saturation model for mAb1. The figure shows particle concentration (a) as a function of both time and (b) reciprocal sample level height. The slope of the lines in (B) represents the saturated surface concentration of particles (larger than two microns) and is approximately 400,000 particles per square centimeter. In samples with the least volume (to the right in (B)), the surface did not saturate during the experiment, leaving the bulk liquid particle free.

$$V(\rho - \rho_w)g = 6\pi\eta rv,$$

where ρ is the particle density, ρ_w is the water density, g equals 9.8 m/s^2 , r is the radius of the particle, η the solution viscosity and v the sedimentation velocity of the particle. The left side of the equation describes the gravity pull and lift, and the right side of the equation is the Stokes drag. The volume of a spherical particle is $V = 4\pi r^3/3$. The final expression for the sedimentation velocity is

Table 1 The Estimation of Total Protein Mass Desorbed from the Rinsed Vials After Incubation with GuHCl

Protein	Sample volume	Vial material	Temperature stress duration (days)	PS80	Recovered protein (mg)
mAb 1	V2	glass	14	y	0,05
mAb 1	V2	PETG	14	y	0,06
mAb 1	V4	PETG	14	y	0,065
mAb 2	V4	PETG	65	y	0,11
mAb 2	V4	glass	65	n	0,075
mAb 2	V4	PETG	65	n	0,09
mAb 2	V5	glass	36	n	0,03
mAb 2	V2	PETG	36	n	0,015
mAb 3	V2	PETG	7	y	0,02
mAb 3	V2	glass	59	y	0,03
mAb 3	V2	PETG	59	y	0,02
mAb 3	V5	glass	59	n	0,01

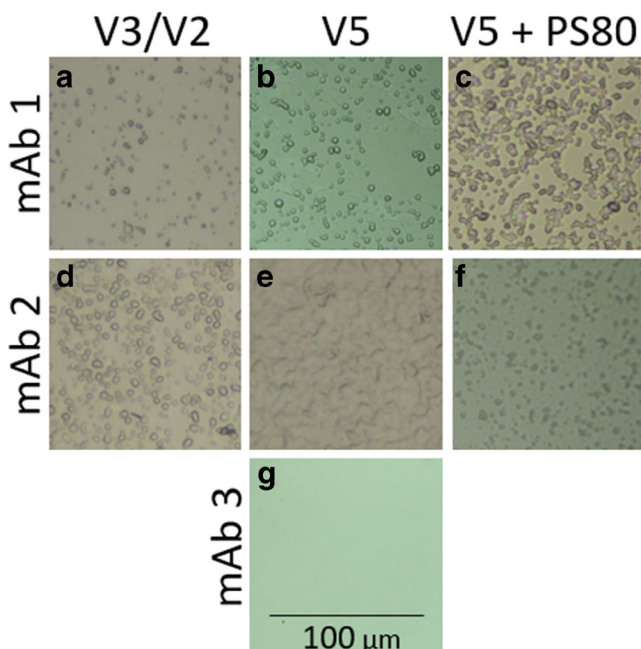


Fig. 6 Effects of vial fill volume and surfactant on particle adhesion, as observed by optical microscopy. Bottoms of vials filled with different volumes of mAb 1 after 14 days of elevated temperature at 40°C (**a** and **b**) were similar regardless of the sample volume. In mAb 2 vials after 2 months at 40°C (**d** and **e**), the surface particle concentration increased with sample volume, with clearly seen overlapping of particles in V5. Surfactant increased the number of particles in mAb 1 (**c**) and decreased it in mAb 2 samples (**f**). The bottoms of MAb 3 vials (**g**), as well as the fresh vials in which the stressed mAb 1 was transferred and stored at 5°C, remained clear even after 2 months.

$$v = \frac{2(\rho - \rho_w)gr^2}{9\eta}$$

Further assuming 80% of the particle to be composed of water, the average particle density ρ amounts to around 1.1 g/cm² rather than the density of pure protein (~1.4 g/cm²) (30). The sample viscosity η is roughly estimated at 1 cP. All of the above assumptions yield the sedimentation velocity in the order of magnitude of 1 mm/h for a particle with the radius of 1 μm (ECD of 2 μm). Depending on the point of origin, size and shape, it takes a micrometer-sized particle hours or days to reach the bottom of the investigated samples. This is much lower than the timescale of the shortest stress stability study (19 days for mAb 1), meaning that most of the particles above 2 μm reached the bottom throughout the experiment, making the sedimentation/adhesion model feasible.

Additional insights can be gained by studying not only the particle concentration, but also particle size distributions (Fig. 7). All of the samples show exponential decrease of particle concentration with size, but with different rates (slopes). Figure 7b shows that all distributions become more biased towards larger particles with time, in addition to the increase in the sole number of particles. That is the result of sedimentation and accumulation of particles near the bottom.

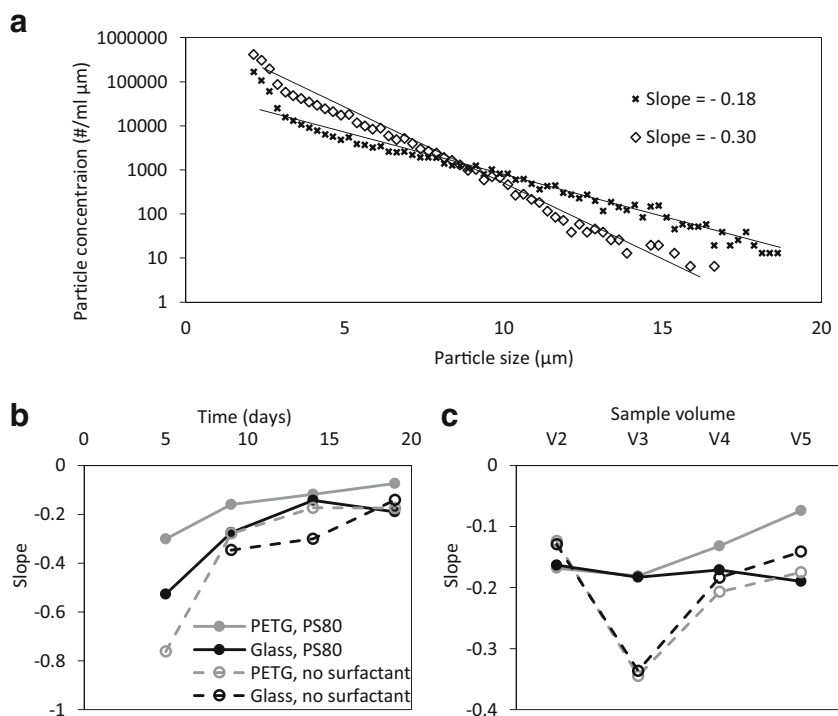
Smoluchowsky type models do not predict such a fast increase in particle size because they assume a homogeneous solution, where large particles are less likely to interact. Figure 7c shows an interesting relation between particle sizes and sample volume. We can see that samples without surfactant with certain volume (both in glass and PETG) tend to contain the smallest particles, while size distributions in samples with surfactant are similar in all the vials. Another important aspect is the similarity between PETG and glass vials. Based on similar values and trends in particle distributions, combined with the desorption study results, we conclude that similar processes of adhesion are present for both materials in all the samples.

For mAb1, the amount of the combined adhered protein material (both coating and particles) in the vials is independent of the filling volume. In contrast, the bottoms of the vials containing mAb 2 samples after elevated temperature stress accumulate more particles in the vials with a larger sample volume – i.e., smaller surface to volume ratio (Fig. 6). MFI measurements do not show an increase of particle concentration in bulk. This means that the surface does not saturate and adhesion of particles is continuous. MAb 3 is stable regarding larger particle formation, with low concentration of particles in bulk solution and with vial bottom essentially free of particles over the course of the experiment.

Temperature Dependence of Adhesion

An important temperature dependence of surface affected protein aggregation is observed from joint conclusions at 40°C and 5°C. While the particles readily adhered at elevated temperature (40°C), this behavior does not necessarily reflect their behavior at realistic storage conditions (5°C), where unexpected accumulation of particles in the bulk is observed, as shown in Fig. 8. Thermally stressed samples of mAb 1 containing large numbers of particles were transferred to fresh vials, incubated at 5°C for a month, and then measured by AFM and MFI. These vials accumulated no particles and had a much thinner protein coating than the vials from the thermal stress (10 nm versus 30 nm). Interesting findings were revealed after re-measuring of selected samples by MFI. Namely, selected mAb 2 and mAb 3 samples, stored after elevated temperature conditions for about 6 months in their original vials at 5°C, were analyzed. MAb 2 without surfactant showed a clear increasing trend in the particle concentration. The impact of this important phenomenon on the stability studies is further discussed below. MAb 3, which did not form any particles (adhered or in bulk) at 40°C, was stable at storage conditions, with all the particle counts much lower than in the mAb 2 case. Only one measurement at 5°C showed an increase compared to the measurements at 40°C.

Fig. 7 Size distributions of particle concentration in mAb 1 samples contained in both glass and PETG vials. **(a)** Exemplary exponential size distributions, described with fitted exponents (slopes). More negative values of the slope mean a heavier bias towards smaller particles. **(b)** Size distribution slopes as a function of temperature stress duration for V5 samples, showing an increase in particle size over time. **(c)** The effect of sample volume on the size distribution after 19 days of temperature stress.



Formation of Smaller Aggregates as Affected by Surface to Volume Ratio

The MFI and AFM data were complemented and compared with SEC measurements. Size exclusion was used to measure aggregates in a very different size range, with the nanometer range for SEC compared to the presented images in micrometer range for optical/atomic force microscopy. All the aggregation peaks of each chromatogram were summed and the aggregation rate was calculated as the relative monthly increase in the sum of aggregation peaks for each formulation by fitting a straight line to the data. Data is presented in Fig. 9a in dependence to surface to volume ratio. This ratio was calculated by the sample volume, measured liquid height and the assumption of a perfect cylindrical shape. Only vial surface was considered, as it is the main variable (glass vs. PETG – the air interface is similar for both types of vials and is not included in the ratio). The rate of smaller aggregate formation varied between proteins. mAb 2 was the most aggregation prone with more than 5% increase in aggregates per month of thermal stress conditions followed by a 0.5% increase per month for mAb 1 and 0.3% increase per month for mAb 3. These data add another dimension to overall protein aggregation propensity, as the rate of formation of smaller aggregates in mAb 2 is an order of magnitude higher than in mAb 1, while the propensity for particle formation of both is quite similar when taken both the surface and bulk measurements into account. On the other hand, SEC measurements of mAb 1 and mAb 3 were quite similar, while mAb 3 was stable regarding larger particle formation. SEC measurements also

uncovered specific protein-surface interactions. Of all the proteins, mAb 2 was the only one that showed a definitive response to both surface to volume ratio as well as vial material. The samples in glass vials with lower volume – higher surface to volume ratio – formed more small aggregates in bulk than the larger volume samples, suggesting specific protein-material interactions that promote aggregation of native monomers. This phenomenon was only apparent in mAb 2 samples in glass vials. It is quantified in Fig. 9b. This is in contrast to the effect of surfaces on larger, subvisible particles, whose concentration is higher in the larger volume samples for mAb 1 (Fig. 5).

Role of Surfactant

The presence of PS80 in the formulation had very mixed effects (i.e. not always reducing particle formation).

With the addition of a surfactant, the bulk concentration of particles in all mAb 1 samples initially increased to a final level, depending on the surface to volume ratio (Fig. 10). Since the concentration of the aggregates in bulk as well as on the surface was consistently higher than in the samples without surfactant (Fig. 6), we conclude that PS80 promotes mAb 1 aggregation, but the underlying mechanism remains unknown.

In the case of mAb 2, the number of adhered particles was much lower in samples containing PS80 (Fig. 6), but the thickness of the uniform coating under the particles increased by two-fold (Fig. 4). At storage conditions at 5°C, surfactant had a positive effect as it prevented accumulation of particles in bulk

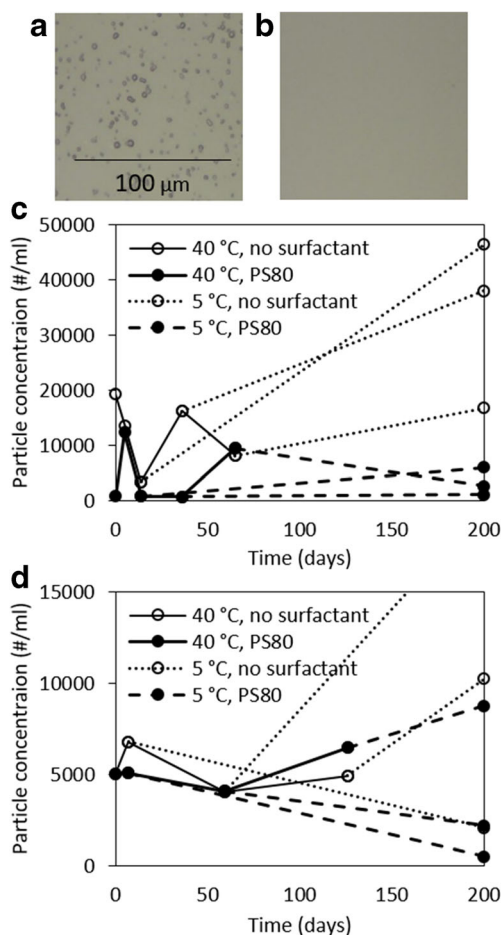


Fig. 8 Temperature effects on adhesion and particle accumulation in bulk. (a) Adhered mAb 1 particles on the vial bottom after 14 days at 40°C (optical microscopy). (b) Bottoms of fresh vials filled with particle-rich samples and stored at 5°C. The existing particles do not adhere to the bottom at storage temperature (optical microscopy). MFI results for (c) mAb 2 and (d) mAb 3. Solid lines represent samples subjected to elevated temperature and dotted/dashed lines represent samples put into storage (original vial) after elevated temperature conditions and remeasured after approximately 6 months. No clear trend can be discerned for samples at elevated temperature, but the same samples remeasured after storage display a definite increasing trend in the case of mAb 2 without surfactant. Mab 3 samples do not show a definite increasing trend at any temperature.

solution (Fig. 8). It is, however, unclear whether the surfactant actually prevented aggregate formation or just promoted adhesion to the surface (now at lower temperature).

Surfactant did not influence formation of smaller aggregates as measured by SEC for any protein.

DISCUSSION

A key requirement for an accelerated stress stability screening of a pharmaceutical product is to ensure drug stability during storage, which in turn ensures the quality and consistency of the drug. From a commercial perspective, 18 months is

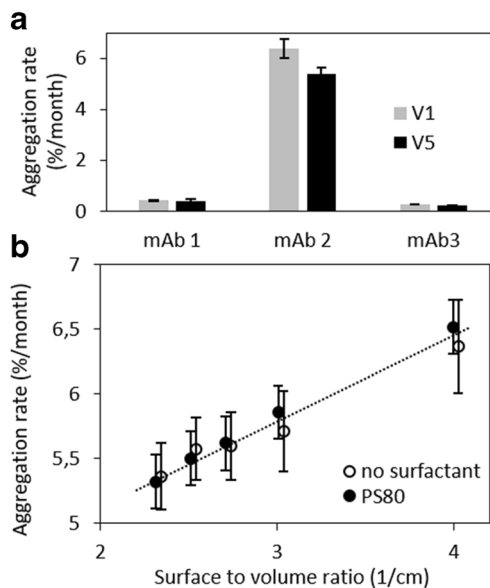


Fig. 9 Rate of formation of smaller aggregates, measured by SEC. (a) Comparison between mAbs in glass vials without PS80. Data for PETG vials are within the measurement error of the presented data, with the exception of: (b) dependence of the rate of aggregation on surface to sample volume ratio for mAb 2 in glass vials. Aggregation rate increases with exposure to a glass surface, but only in mAb 2 samples. The same samples in PETG vials do not show any dependence on the sample volume.

frequently the minimally acceptable shelf life due to the time required for production, packaging, and distribution. In contrast, initial stability screenings at elevated temperature, which play a significant role in formulation selection, take a couple of months at most. Therefore, characterization of particle formation mechanisms, particle adhesion, specific protein-surface interaction and the effect of surfactant are all of major importance for the pharmaceutical industry.

We have demonstrated that container surface material and surface to volume ratio, in combination with different proteins and at different external conditions (temperature, surfactant), can strongly affect aggregation behavior. Moreover, some particle formation processes at elevated temperature can be hard to detect if performing only standard screening tests. In a typical stability screening setting only particles in bulk solution

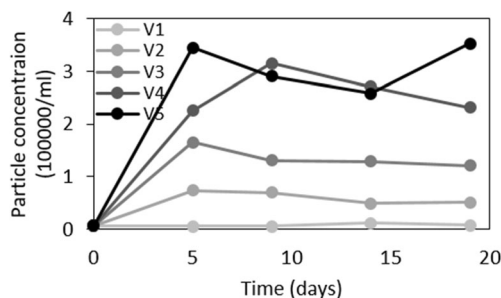


Fig. 10 Surfactant effect on mAb 1 bulk particle concentration (MFI). With surfactant, the particle concentration increases sharply and reaches a plateau, which is higher in samples with larger volume.

are analyzed, either by flow imaging or by light obscuration methods, but a chosen formulation may promote aggregation which remains undetected due to adhesion of aggregates to the surfaces of the container. We also show that particle surface adhesion appears to be temperature dependent, which could lead to discrepancies between stability screenings at different temperatures. As seen in the case of mAb 1, the particles formed at higher temperature do not adhere to a fresh vial under storage conditions at 5°C. In the case of mAb 2, particles are present in bulk solution of samples without surfactant after approximately 6 months under storage conditions, which is in contrast to the elevated temperature stressed samples where no increase in bulk particle concentration could be determined. Based on particle formation propensity of mAb 2 as determined from AFM and the apparent temperature dependence of adhesion as measured in mAb 1, we predict that the particles still form, albeit at a lower rate, but do not adhere to the vial at lower temperatures. The same mAb2 formulations with surfactant do not contain significantly more particles in bulk solution after long term storage conditions, indicating that the surfactant either prevents aggregate formation or just promotes adhesion even at lower temperature. Most importantly, in these experiments the accelerated stress conditions are *not* representative for considering the bulk particle formation under storage conditions. These results raise additional questions about actual long-term particle-reducing mechanism of surfactants in biologics and furthermore, the necessity of special low binding protein containers as a possible choice for primary packaging of biologics – adhesion of particles is actually a desired effect, as such particles ultimately never reach the patient. In all the tested cases the total amount of surface adhered material is negligible compared to total protein material in the vial, with the loss of native protein material in the bulk undetectable by UV methods (< 1%). Potency is thus not affected, with the potential risk to the patients due to protein aggregates greatly reduced.

CONCLUSION

High variability in particle behavior among different mAbs presented in this study shows the importance of individualized screening approaches, which are currently also of direct interest to biopharmaceutical industry. We further stress the limitations of common methods for particle characterization in bulk solution, such as LO or MFI, used in such screenings, which are shown to be insufficient for assessing surface affected protein aggregation. We show that adhesion of particles to vial surfaces at elevated temperature stress can mask particle formation propensity when assessed by standard combinations of methods, potentially leading to a selection of a formulation which is unstable at intended storage conditions. Specifically, special notice has to be taken when interpreting particle count

data from stability studies when different temperatures and vial types are involved. Therefore, if formulation selection is based on LO or MFI measurements, container surfaces should also be thoroughly checked for particles. Finally, this work contributes to the development of biopharmaceutics by evaluating current practices in a critical manner and pointing out deficiencies which could potentially lead to development of unstable formulations.

ACKNOWLEDGMENTS AND DISCLOSURES

M.R. acknowledges funding from Lek Pharmaceuticals d.d. under contract BIO17/2016 and from Slovenian Research Agency ARRS grants L1-8135, P1-0099, and P1-0340. M.Z. and D.K. acknowledge funding from program BioPharm.Si project co-funded by Republic of Slovenia - Ministry of Education, Science and Sport - and European union - European regional development fund.

Publisher's Note Springer Nature remains neutral with regard to jurisdictional claims in published maps and institutional affiliations.

REFERENCES

- Vazquez-Rey M, Lang DA. Aggregates in monoclonal antibody manufacturing processes. *Biotechnol Bioeng.* 2011;108:1494–508.
- Kueltzo LA, Wang W, Randolph TW, Carpenter JF. Effects of Solution Conditions, Processing Parameters, and Container Materials on Aggregation of a Monoclonal Antibody during Freeze-Thawing. *J Pharm Sci.* 2008;97:1801–12.
- Sathish JG, Sethu S, Bielsky MC, de Haan L, French NS, Govindappa K, *et al.* Challenges and approaches for the development of safer immunomodulatory biologics. *Nat Rev Drug Discov.* 2013;12(4):306–24.
- Chi EY, Krishnan S, Randolph TW, Carpenter JF. Physical stability of proteins in aqueous solution: mechanism and driving forces in nonnative protein aggregation. *Pharm Res.* 2003;20(9):1325–34.
- Cohen SLA, Vendruscolo M, Dobson CM, Knowles TPJ. From macroscopic measurements to microscopic mechanisms of protein aggregation. *J Mol Biol.* 2012;421:160–71.
- Ratanji KD, Derrick JP, Dearman RJ, Kimber I. Immunogenicity of therapeutic proteins: Influence of aggregation. *J Immunotoxicol.* 2014;11(2):99–109.
- Fathallah AM, Chiang M, Mishra A, Sandeep K, Xue L, Middaugh CR, *et al.* The Effect of Small Oligomeric Protein Aggregates on the Immunogenicity of Intravenous and Subcutaneous Administered Antibodies. *Pharm Biotechnol.* 2015;104:3691–702.
- Wang X, Das KD, S. K S, Kumar S. Potential aggregation prone regions in biotherapeutics. *mAbs.* 2009;1(3):254–67.
- Arosio P, Rima S, Morbidelli M. Aggregation Mechanism of an IgG2 and two IgG1 Monoclonal Antibodies at low pH: From Oligomers to Larger Aggregates. *Pharm Res.* 2013;30:641–54.
- Brummitt RK, Nesta DP, Chang L, Chase SF, Laue TM, Roberts CJ. Nonnative Aggregation of an IgG1 Antibody in Acidic Conditions: Part 1. Unfolding, Colloidal Interactions, and Formation of High-Molecular-Weight Aggregates. *J Pharm Sci.* 2011;100:2087–103.

11. Yageta S, Lauer TM, Trout BL, Honda S. Conformational and Colloidal Stabilities of Isolated Constant Domains of Human Immunoglobulin G and Their Impact on Antibody Aggregation under Acidic Conditions. *Mol Pharm*. 2015;12:1443–55.
12. Barnett GV, Drenski M, Razinkov V, Reed WF, Roberts CJ. Identifying protein aggregation mechanisms and quantifying aggregation rates from combined monomer depletion and continuous scattering. *Anal Biochem*. 2016;511:80–91.
13. Kim N, Remmele RL Jr, Liu D, Razinkov VI, Fernandez EJ, Roberts CJ. Aggregation of anti-streptavidin immunoglobulin gamma-1 involves Fab unfolding and competing growth pathways mediated by pH and salt concentration. *Biophys Chem*. 2013;172:26–36.
14. Imamura H, Honda S. Kinetics of Antibody Aggregation at Neutral pH and Ambient Temperatures Triggered by Temporal Exposure to Acid. *J Phys Chem B*. 2016;120:9581–9.
15. Nicoud L, Arosio P, Sozo M, Yates A, Norrant E, Morbidelli M. Kinetic Analysis of the Multistep Aggregation Mechanism of Monoclonal Antibodies. *J Phys Chem B*. 2014;118:10595–10,606.
16. Smoluchowski M. Drei Vorträge über Diffusion, Brownsche Molekularbewegung und Koagulation von Kolloidteilchen. *Zeitschrift für Physik*. 1916;17:557–71, 585–599.
17. Wattis JA. An introduction to mathematical models of coagulation–fragmentation processes: A discrete deterministic mean-field approach. *Phys D*. 2006;222:1–20.
18. Kryven I, Lazzari S, Storti G. Population Balance Modeling of Aggregation and Coalescence in Colloidal Systems. *Macromol Theory Simul*. 2014;23:170–81.
19. Koepf E, Schroeder R, Brezesinski G, Friess W. The film tells the story: Physical-chemical characteristics of IgG at the liquid-air interface. *Euro J Pharm Biopharm*. 2017;119:396–407.
20. Ghazvini S, Kalonia C, Volkin DB, Dhar P. Evaluating the Role of the Air-Solution Interface on the Mechanism of Subvisible Particle Formation Caused by Mechanical Agitation for an IgG1 mAb. *J Pharm Sci*. 2016;105:1643–56.
21. Shieh IC, Patel AR. Predicting the Agitation-Induced Aggregation of Monoclonal Antibodies Using Surface Tensiometry. *Mol Pharm*. 2015;12:3184–93.
22. Mehta SB, Lewus R, Bee JS, Randolph TW, Carpenter JF. Gelation of a Monoclonal Antibody at the Silicone Oil-Water Interface and Subsequent Rupture of the Interfacial Gel Results in Aggregation and Particle Formation. *Pharm Biotechnol*. 2015;104:1282–90.
23. Sediq AS, Duijvenvoorde RBV, Jiskoot W, Nejadnik MR. No Touching! Abrasion of adsorbed protein is the root cause of subvisible particle formation during stirring. *J Pharm Sci*. 2016;105:519–29.
24. P. T, N. H, N. DP and R. CJ, “Protein Adsorption, Desorption, and Aggregation Mediated by Solid-Liquid Interfaces,” *Pharm Biotechnol*. 2015;104, (6), 1946–1959.
25. X. H, Z. X, G. C and L. JR, “Orientation of a Monoclonal Antibody Adsorbed at the Solid/Solution Interface: A Combined Study Using Atomic Force Microscopy and Neutron Reflectivity,” *Langmuir*. 2006;22, (14), 6313–6320.
26. F. CW and W. ME, “Antibody adsorption and orientation on hydrophobic surfaces,” *Langmuir*. 2012; 28, (3), 1765–1774.
27. Randolph TW, Schiltz E, Sederstrom D, Steinmann D, Mozziconacci O, Schoneich C, *et al*. Do not drop: mechanical shock in vials causes cavitation, protein aggregation, and particle formation. *Pharm Biotechnol*. 2015;104:602–11.
28. Torisu T, Maruno T, Hamaji Y, Ohkubo T. Synergistic Effect of Cavitation and Agitation on Protein Aggregation. *J Pharm Sci*. 2017;106:521–9.
29. Wang S, Wu G, Zhang X, Tian Z, Zhang N, Hu T, *et al*. Stabilizing two IgG1 monoclonal antibodies by surfactants: Balance between aggregation prevention and structure perturbation. *Euro J Pharm Biopharm*. 2017;114:263–77.
30. Kalonia C, Kumru OS, Prajapati I, Mathaes R, Engert J, Zhou S, *et al*. Calculating the Mass of Subvisible Protein Particles with Improved Accuracy Using Microflow Imaging Data. *Pharm Biotechnol*. 2015;104(2):536–47.
31. M. Zidar, D. Kuzman and R. M, “Characterisation of protein aggregation with the Smoluchowski coagulation approach for use in biopharmaceuticals,” *Soft Matter*. 2018; 14, 6001–6012.

Publisher’s Note Springer Nature remains neutral with regard to jurisdictional claims in published maps and institutional affiliations.